Carbonates Evaporites (2017) 32:525–537
DOI 10.1007/s13146-016-0309-2

ORIGINAL ARTICLE

Hydrothermal dissolution of Ordovician carbonates rocks and its dissolution mechanism in Tarim Basin, China

L. H. Liu[1,2] · Y. S. Ma[1,3] · B. Liu[1] · C. L. Wang[4]

Accepted: 27 April 2016 / Published online: 23 July 2016

Abstract The dissolution of carbonate rocks has a significant control on reservoir quality under deep burial conditions, which has become a focus of studies in recent years. A series of hydrothermal minerals and combinations, such as fluorite, dickite, barite and hydrothermal dolomite, were discovered in the Ordovician strata in some exploration wells in the Tahe area. Moreover, the analysis results of carbon and oxygen isotope, REE, strontium isotope and inclusion homogenization temperature further confirmed that hydrothermal fluids existed in the Ordovician strata of Tahe areas. In this paper, the dissolution mechanism of carbonate rocks under deep burial conditions is discussed. It was considered that the hydrothermal dissolution required three conditions, i.e., the development of fault system, the presence of acidic fluids and a fall in temperature. The major theoretical foundation was the retrograde solubility of carbonate rocks that could be achieved through temperature drop and the upward migration of hydrothermal fluids. The dissolution of carbonate rocks caused by hydrothermal fluids normally occurred in the vicinity of migration pathways (faults or other pathways), which could be identified as good reservoir development zones.

Keywords Tarim Basin · Deep buried · Retrograde solubility · Hydrothermal fluid · Carbonates reservoirs

Introduction

Extensive studies show that the greater the burial depth, the lower is the porosity, for either clastic or carbonate rocks. Empirical data suggest that the porosity is decreased by 1–3 % per km (Ehrenberg and Nadeau 2005). In theory, reservoirs should not be developed in deeply buried units. However, with the exploration of deeply buried basins, there have been numerous discoveries of oil and gas reservoirs, in deep and ultra-deep carbonate strata, such as the Tahe oilfield in the Tarim Basin, and the Puguang, Yuanba, Longwangmiao and Dengying oil and gas fields in eastern Sichuan. These large oil and gas fields occur at depths of over 5000 m (Ma et al. 2011). These discoveries reveal that deeply buried carbonate rocks, especially dolomite, can be host to valuable reservoir space. Understanding the processes and conditions that lead to the formation and development of oil and gas reservoirs under deep burial conditions is of great theoretical and practical significance for oil and gas exploration in deeply buried zones.

Thus far, only a few of studies have been conducted on deep reservoir formation mechanism in China (Zhu et al. 2008; Pan et al. 2009). Huang et al. (2010b) considered that the reservoir development under deep burial conditions was closely related to the dissolution of carbonate rocks during burial diagenesis. Huang et al. (2010b) suggest, based on geological evidence and thermodynamics, that

✉ C. L. Wang
wangchunlian312@163.com

[1] Oil and Gas Research Center, School of Earth and Space Sciences, Peking University, Beijing 100871, China

[2] Oil & Gas Survey, China Geological Survey, Beijing 100029, China

[3] Oilfield Exploration and Production Department, Sinopec, Beijing 100728, China

[4] MLR Key Laboratory of Metallogeny and Mineral Assessment, Institute of Mineral Resources, Chinese Academy of Geological Sciences, Beijing 100037, China

carbonate dissolution would occur as tectonic uplift and ascending diagenetic fluids via faults, resulting in cooling down of fluid and thereby undersaturation with respect to carbonate. This process has been inferred for the Tarim Basin by various researchers (e.g., Zhu et al. 2008; Jin et al. 2006; Wang et al. 2004; Zhang et al. 2006). Similar processes have been implied in the development of high-quality reservoirs in the middle Devonian Western Canada sedimentary basin (Ihsan and Aasm 2002).

In this paper, core descriptions, thin section petrography and SEM analysis are used to identify petrological and mineralogical features resulting from hydrothermal process of a few wells cored in the Tahe area of the Tarim Basin. Geochemical analyses were carried out on these materials and include carbon and oxygen isotopes, REE, strontium isotopes and fluid inclusion homogenization temperatures, and used to characterize the hydrothermal fluids in the Tarim Basin. Moreover, new hydrothermal dissolution mechanisms are proposed and their impact on hydrothermal dissolution on carbonate reservoirs is discussed.

Geological setting

The Tarim Basin is located south of the South Tianshan Mountains (Fig. 1), northwest China. The study area is the Tahe oilfield, which is located on the northern portion of the Tarim Basin. The Tahe oilfield was the first field in the Tarim Basin, producing oil from marine strata (Kang 2005). The majority of the production is from the Ordovician strata consisting of shallow platform and slope facies carbonate. The Ordovician strata in this area comprised six formations, from oldest to youngest these are the Penglaiba, Yingshan, Yijianfang, Qiaerbake, Lianglitag and Sangtamu formations, from lower to upper. The lithology is described in Table 1.

Structurally, the Tahe oilfield is located in the southwest slope of the Akekule thrust of the Shaya uplift of the Tarim Basin. The Ordovician sequence experienced multi-stage tectonic movement, of which the middle Jialidong (late Ordovician to early Silurian; e.g., Liu et al. 2012) event and Heisey (Devonian to Permian; e.g., Charvet et al. 2007) events are the most important. The uplift during the middle Jialidong changed the sedimentary facies of the Tarim Basin from pure marine carbonates to mixed clastic carbonates or muddy clastic sediments (Table 1). The carbonate reservoirs of the middle Ordovician Yijianfang Formation are predominantly reef (algal) and shoal (ooids), and the upper Ordovician Lianglitag Formation reservoirs are mostly of algal and reef/buildups (Kang 2005).

Exposure and erosion of the carbonates of the Yijiangfang and upper Lianglitag formations correspond to two distinct times in which the sea level decreased during the middle Jialidong movement. The upper Ordovician Qiaerbake and Sangtamu formations were deposited during episodes of global sea level rise. The early Heisey

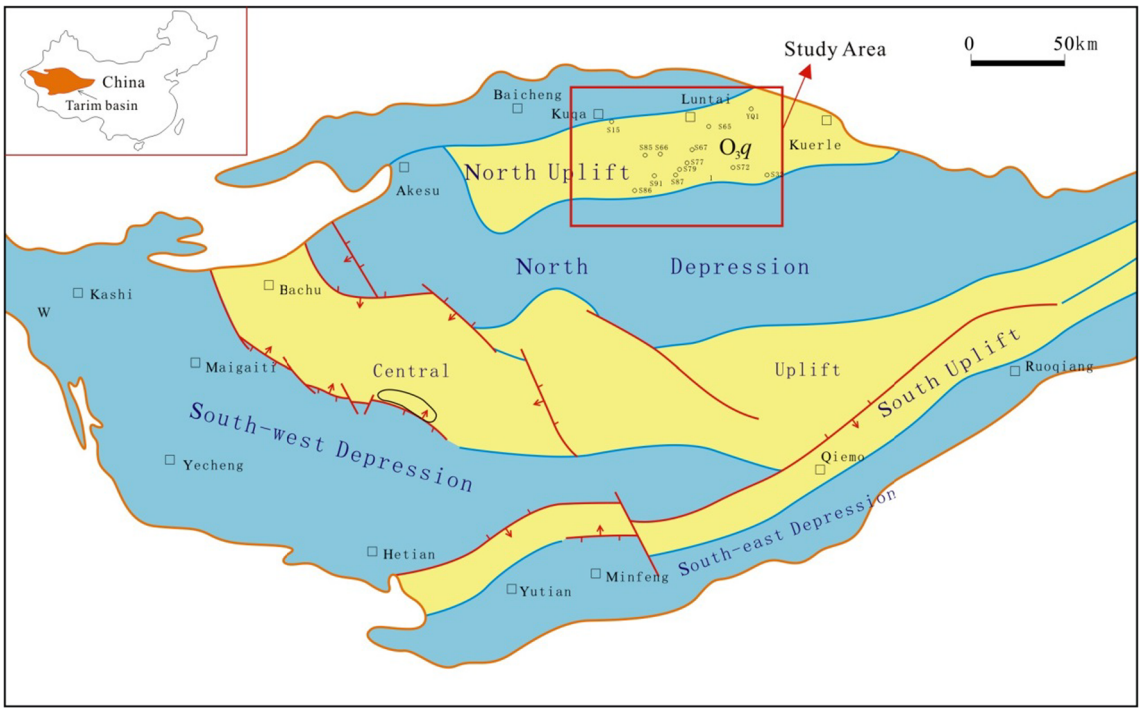

Fig. 1 Geology of the Tarim Basin region (modified from PetroChina)

Table 1 The table of Cambrian–Ordovician strata of the Tahe oilfield

Strata					Wave	Thickness (m)	Lithology
E	S	S	F	Mark			
					T_7^0		
O		Upper	Sangtamu	O_3s		0–600	Upper: grey green-dark brown silty mudstone interbedded with dolomitic mudstone or dolomite, local bioclast limestone and oolitic limestone. Lower: grey micrite limestone and silty mudstone interbedding
			Lianglitag	O_3l		0–120	Grey, dark grey and brown grey micrite limestone, calcirudyte, oolitic limestone, local small scale organic reef
			Qiaerbake	O_3q		0–25	Grey red, purplish red, brown grey muddy limestone, bioclast limestone interbedded with brownish red mudstone
		Middle	Yijianfang	O_2yj	T_7^4	0–80	Grey, brown grey calcarenite, bioclast limestone, oolitic limestone, micrite limestone-power crystal limestone, small scale organic reef
			Yingshan	$O_{1\text{-}2}y$		600–900	Upper: light grey micrite limestone, bioclast micrite limestone, micrite calcarenite interbedded; Lower: micrite dolomite, micrite calcarenite interbedded with light grey dolomitic limestone, limy dolomite and dolomite
		Lower	Penglaiba	O_1p		250–400	Light grey dolomite, limy dolomite interbedded with dolomitic limestone
	C	Upper	Qiulitage	$\in_3$ql	T_8^0	1000–1500	Light grey micro-crystal power dolomite interbedded with sand sized-oolite dolomite, algae dolomite
Underlayer				$\in_2$			

movement caused extensive karst dissolution of the early Paleozoic carbonates, giving rise to the dominant reservoirs in Ordovician carbonates in the north of the Tahe oilfield (Yu 2006).

This study focuses on the Cambrian and Ordovician carbonates (Table 1), in which the Cambrian strata are light gray to reddish-gray massive to medium bedded. The dolomite consists of fine–medium size crystals, algae, stromatolites, and ooids which are all dolomitized, and in places detrital ravel to sand-sized dolomite is found. In places, dolomitized oolites are interbedded with siliceous lenses. The total thickness of Cambrian is 320–400 m. In the Tahe area, only one well, TS1, penetrated the lower Qiulitage.

Materials and methods

Samples were collected from cores of the S85, S88, S15, S65, and TS1 wells. Thin section samples were used for petrographic examination, doubly polished slabs were used of fluid inclusions temperature measurements, and powder samples were extracted for elemental REEs, carbon–oxygen, and strontium isotope analyses. The calcite in pores and cavities were sampled by micro drill to separate it from surrounding rock. Then the samples were crushed into small pieces of several millimeters, and further ground into powder less than 200 meshes in agate mortar for the purpose of REE and isotope analyses.

The element composition is obtained through EPMA-1600 at the Southwest Mineral Resources Supervision and Inspection Center of Ministry of Land and Resources. When analyzing, the voltage was 15kv and current 20 nA. Fluid inclusion temperature measurements were carried out on a Linkam Coo1ing System THMS600 in the State Key Laboratory of Chengdu University of Technology. The precision of temperature measurement is ±1 °C. The carbon and oxygen isotope analysis was carried out on MAT252 Gas Isotope Ratio Mass Spectrometer in the Geological Laboratory of PetroChina Southwest Oil and Gasfield Company. Strontium isotope analysis was conducted in the Institute of Geology and Geophysics of Chinese Academy of Sciences.

Results

Petrographic evidence

Hydrothermal fluid migration along faults and fractures resulted in the precipitation of a variety of minerals, such as fluorite, dickite, barite and dolomite. The precipitation of these minerals resulted from changes in temperature and pressure, as fluids ascended and chemical changes took place as they interacted with the surrounding rocks.

Presence of fluorite

There is a lot of controversy about the genesis of fluorite ore in this region. Most scholars (Zhu et al. 2008; Wang et al. 2004) considered that fluorite ore was derived from magmatism and its formation was related to the Hercynian–Late Permian magmatic thermal events that occurred in the Tarim Basin. However, other scholars argued that the ore-forming hydrothermal fluids were derived from heated meteoric waters (Zhang et al. 2006; Pan et al. 2012). We have observed fluorite along fractures in the Yingshan Formation in the S65 well (Fig. 3a). Fluorite in the

Yijianfang Formation in the S85, S76 and S86 wells has also been reported by others (e.g., Li et al. 2008). Analysis of the fluid inclusions homogenization temperatures showed that the temperature of fluorite precipitation in the Yijianfang Formation in the S85 well was high, with a narrow range from 208.5 to 218.5 °C, and an average of 213.6 °C (Table 2). This range is higher than the expected temperature of 201 °C if we assume a geothermal gradient of 3 °C/100 m and surface temperature of 25 °C. Fluorite is thus considered to be of hydrothermal origin.

Presence of dickite

Dickite is widely distributed in various hydrothermal sedimentary rocks, but it is rarely present in carbonate formations. Huang et al. (1995) reported that dickite was widespread on the top of Ordovician paleo-weathering crusts in the Ordos Basin. Zhao (1997) reported dickite presence in the Lower Ordovician weathering crust in the southwestern Tarim Basin. The provenance of dickite in the above occurrences was related to weathering and most likely it was converted from kaolinite (Huang et al. 1995).

Dickite was found at 6408.79 m in the S88 well in the Tabei area, identified by its hexagonal-platelet morphology with assemblages in booklet or pillared layered morphology as seen in SEM (Fig. 3c, d) and X-ray diffraction pattterns (Fig. 2). The dickite discovered in the S88 well was far away from the Ordovicians exposure unconformity and 925 m below the closest overlying erosional unconformity (i.e., the surface between the carboniferous Bachu Formation/Ordovician Yingshan Formation). Cleary, the dickite origin in the S88 well was unrelated to low-temperature weathering or conversion from kaolinite during the burial diagenetic process. Furthermore, the dickite discovered in the S88 well occurred in brecciated limestone (Fig. 3c, d), suggesting that its origin was associated with the hydrothermal activity producing the breccias. It is likely that the dickite might be associated with the deep hydrothermal fluids that went through strata rich in aluminum silicates.

Presence of barite

Pore-filling barite is found at the same depth as fluorite in the Yingshan Formation in the S65 well (Fig. 3b). Barite has been reported in other localities of the Tarim Basin, such as in the Tazhong 4 well at a depth of 3609.96 m (Jin et al. 2006) and in the Tazhong 12 well (Cai et al. 2009; Li et al. 2008). The barite involved in this study showed fasciculate shape, with a set of cleavage extensively distributed in the long axis direction. It is Sr rich, with BaO and SO_3 content of 63.47 and 35.76 %, respectively, and SrO content as high as 0.62 %. The association of barite and fluorite supports pervasive hydrothermal activity in the Tahe area.

Presence of saddle dolomite

The dolomitization (or recrystallization of dolomite) under high temperature resulted in the loss of original

Table 2 Homogenization temperature of the primary brine inclusions in fluorite in the S85 well (5872.24 m)

Size (μm)	3	3	3	3	2	2	4	3	4	2	3	3	T_h average value (°C)
Gas–liquid ratio (%)	3	5	5	5	5	8	3	8	5	5	5	10	
T_h(°C)	208.5	209.3	209.6	211.4	211.7	213.4	213.6	213.9	216.8	217.6	218.4	218.5	213.6

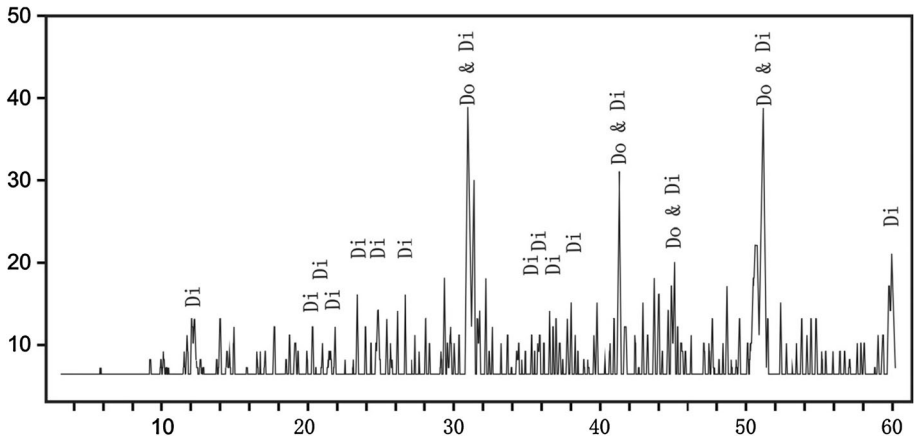

Fig. 2 X-ray diffraction graph of the dickite sample. *Di* is the X-ray diffraction of dickite and *Do* is that of dolomite, most of which is not marked. 6408.79 m, S88 well

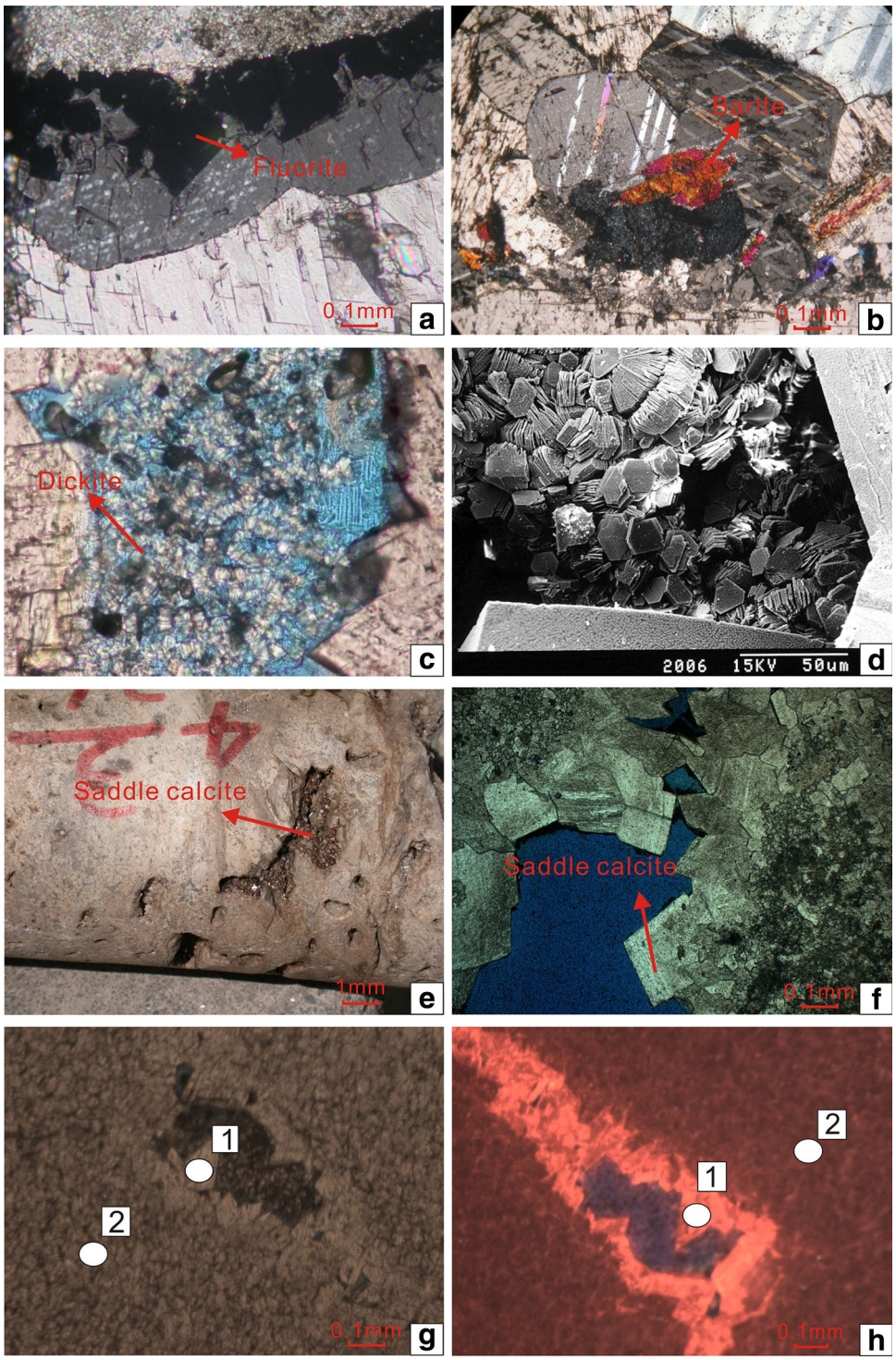

Fig. 3 Photomicrographs of the Ordovician hydrothermal mineral assemblages, Tarim Basin. **a** Fluorite, S65 well, 5475.59 m, Yingshan Formation, **b** barite, S65 well, 5475.59 m, Yingshan Formation, **c** Dickite, S88 well, 6408.79 m, Penglaiba Formation, **d** SEM photo of figure (**c**), **e** dolomite in cavities, TS1, 7875.7 m, Lower Qiulitage Formation, Cambrian, **f** thin section of (**e**), casting section, **g** fine crystal dolomite and crystallized coarse dolomite, point **1** and point **2** is the electron probe test point with result shown above, S88 well, 6408.79 m, Penglaiba Formation, **h** the cathode luminescence of (**g**) with test condition of 326 μA, 16.3 kV

fabric, which has been reported before (Machel 2005). The dolomite can be divided into two types replacement dolomite (mostly non-planar anhedral dolomite) and primary crystals precipitated in vuggy porosity or fabric destructive (mostly euhedral to subhedral crystals). The replacement dolomite is mostly found in shallower systems associated with erosional surfaces. The pore filling or fabric-destructive dolomite is mainly found deeper and probably formed under deep burial conditions (Huang et al. 2009). In the Tahe area, the fabric-retentive replacement dolomite is found in the shallower strata of the Yijianfang and Yingshan formations. The pore-filling

Table 3 Trace element composition of different structures of dolomite in the S88 well

Elements	MgO	CaO	CO_2	MnO	FeO	SrO
Point 1	21.268	30.162	48.514	0.033	0.009	0.007
Point 2	21.231	30.038	48.692	0.001	0.026	0.007

dolomite is found in the deep strata of the Penglaiba Formation, such as in S88 and S15 wells and Qiulitage Formation in the TS1 well. Vuggy porosity is often found in the Penglaiba Formation in the S88 and S15 wells and the Qiulitage Formation in the TS1 well (Fig. 3e, f). Fine to coarse crystalline saddle dolomite fills the pores and is often associated with fluorite (Fig. 3g, h). The saddle dolomite in the pores is generally brightly luminescent with relatively high Mn content (256 ppm) and low Fe content (70 ppm) (Fig. 3e, point 1 and Fig. 3h, Table 3). The matrix commonly has low Mn content (8 ppm) and high Fe content (202 ppm) (Fig. 3e, Table 3, point 2). Dogtooth dolomite in samples, collected 924.79 m away from unconformity, is brightly luminescent suggesting precipitation from non-meteoric or non-marine fluids, and most likely formed in deep buried conditions.

Geochemical evidence

The hydrothermal activity along faults and fractures not only left its trace through the precipitation of a variety of hydrothermal minerals, but hydrothermal fluids also reacted with the carbonate host rocks resulting in alteration of the host rock that can be traced by geochemical changes.

Fluid inclusion homogenization temperatures

The Tarim Basin had experienced several major tectonic events, including the tectonic uplift and subsidence in the Early Paleozoic (Wu et al. 2009) and rapid subsidence since Cretaceous. For most of the basin, the current burial depth is the greatest that the basin has experienced in its geological history (Chen et al. 2009). Based on the burial-thermal history of the Tahe area (Ye 1994), the Ordovician carbonates in the study areas experienced the deepest burial depth and the highest burial temperature (Wu et al. 2012). Present-day burial temperature of the limestone in the sampling location (6400 m in the S88 well) is estimated at 145 °C using a present-day geothermal gradient of 3 °C/100 m and surface temperature of 25 °C. The average measured homogenization temperatures are within this range. However, the maximum measured homogenization temperatures of fluid inclusions are as high as 193.6 °C for calcite and 158.4 °C for dolomite (Table 4), which can only be reached by hydrothermal alteration.

Stable carbon and oxygen isotope evidence

Oxygen isotope fractionation between calcite and fluid occurred during the enriching in the precipitation process (Goldstein and Jacobsen 1987). The oxygen isotopic composition of calcite and fluid was controlled by the temperature of precipitation and the fluid composition. The oxygen isotopic composition of diagenetic calcite is generally light, indicating that diagenetic fluids were either depleted, temperatures were high or a combination of both (Jay and Kevin 1989). We plot the $\delta^{18}O$ and $\delta^{13}C$ value of different components in the S65 and S88 wells (Fig. 4; Table 5). The results show that the calcite in cavities commonly have low $\delta^{18}O$ value, on average less than −11 ‰ (PDB). In the S88 well, the $\delta^{18}O$ value of cavity calcite is only −12.68 ‰ (PDB) at a depth of 6408.79 m where dickite was discovered (Fig. 4b). Although most samples are collected close to the unconformity surface, the meteoric water might cause the light oxygen isotopic composition. All the calcite inclusion had an average homogenization temperature of over 120 °C (Table 4; Fig. 5), which could exclude the influence of meteoric water.

The fluid inclusion homogenization temperatures constrain precipitation temperatures and provide the means to identify the composition and source of diagenetic fluids (Fig. 5). The isotopic composition and fluid inclusion temperatures of Ordovician carbonate require that the $\delta^{18}O$ value of diagenetic fluid should be enriched with values well above those of meteoric fluids and even seawater. While precise salinity measurements are lacking for the fluid inclusion, the limited data suggest salinity certainly higher than that of modern seawater (Ren et al. 2000). Therefore, we conclude that the calcite in Ordovician carbonates was formed under high temperature and high salinity fluids. The source of these fluids is either seawater modified through rock–water interactions with magmatic rocks or was magmatic or metamorphic fluids.

Rare earth elements

Rare earth elements (REEs) have been widely applied for the identification of the source and the study of geochemical behavior of geological bodies and oil and gas reservoirs (Condie 1991). REEs are a powerful tool to track fluid activities in deep zone. Previous studies (Lv et al. 2007; Ding et al. 2000; Zhu et al. 2013; Liu and Cai 2009) revealed that a positive Eu anomaly could be used as an

Table 4 Homogenization temperature of Ordovician carbonate inclusions in some wells in the Tahe region

Well	Depth (m)	Formation	Mineral	From unconformity (m)	$\delta^{18}O$ (‰)	$\delta^{13}C$ (‰)	Homogenization temperature (°C)			
							Average	Max	Min	Samples
S15	5389.8	Penglaiba	Dolomite		−6.09	−1.69	124.1	187.5	53.2	10
S15	5442.7	Penglaiba	Dolomite		−9.16	−3.41	132.6	158.9	111.5	10
S15	5451.9	Penglaiba	Dolomite		−4.64	−1.29	140.3	176.1	113.1	4
S65	5462.8	Yingshan	Calcite	11.8	−11.73	−5.8	162	199.8	134.2	11
S65	5462.8	Yingshan	Calcite	11.8	−7.68	−1.36	86.2	105.2	62.3	6
S65	5475.6	Yingshan	Calcite	24.6	−9.39	−2.07	141.5	157	126	2
S65	5475.6	Yingshan	Calcite	24.6	−12.04	−8.72	137.2	145.1	125.5	5
S65	5532.8	Yingshan	Calcite	81.8	−12.19	−3.37	132.4	173.7	105.2	7
S67	5590.4	Yingshan	Calcite	131.4	−13.22	−2.93	99.1	113.7	69.1	14
S67	5644.6	Yingshan	Calcite	208.1	−10.59	−2.47	111.8	150.1	70.3	10
S65	5733.2	Yingshan	Calcite	282.2	−11.01	−0.54	120.1	185	65	10
S86	5812.6	Penglaiba	Calcite	127.1	−6.89	−0.19	168.5	215.8	115	15
S88	6408.8	Penglaiba	Calcite		−12.68	−3.96	141.4	193.6	93.7	12
S88	6428.2	Penglaiba	Dolomite		−8.66	−1.63	136.8	158.4	117	10

Table 5 The isotope composition of different components of Ordovician carbonate in the S65 and S88 well of the Tahe oilfield

Well	Depth (m)	Samples	Lithology or occurrence	From unconformity (m)	Formation	$^{87}Sr/^{86}Sr$	$\delta^{13}C$ (‰)	$\delta^{18}O$ (‰)	Dolomite (%)
S65	5462.84	S65-21	Calcite in cavities	11.84	Yingshan	0.709374	−5.8	−11.73	0.91
S65	5462.84	S65-21	Sparry grainstones	11.84	Yingshan	0.70876	−1.36	−7.68	2.43
S65	5468.25	S65-19	Sparry grainstones	17.25	Yingshan	0.708778	−1.32	−8.4	0.53
S65	5468.25	S65-19	Calcite in cavities	17.25	Yingshan	0.709373	−15.25	−12.6	7.38
S65	5469.57	S65-18	Micrite grainstones	18.57	Yingshan	0.708755	−0.78	−7.63	0.91
S65	5469.57	S65-18	Sparry grainstones	18.57	Yingshan	0.708925	−0.46	−7.95	3.04
S65	5475.59	S65-15	Calcite in cavities	24.59	Yingshan	0.709382	−8.72	−12.04	0.38
S65	5475.59	S65-15	Micrite grainstones	24.59	Yingshan	0.708946	−2.07	−9.39	3.04
S65	5489.22	S65-12	Sparry grainstones	38.22	Yingshan	0.708761	−0.57	−7.92	1.83
S65	5532.79	S65-10	Calcite in cavities	81.79	Yingshan	0.709417	−3.37	−12.19	1.83
S65	5532.79	S65-10	Micrite limestone	81.79	Yingshan	0.708998	−1.79	−9.87	3.27
S65	5541.49	S65-6	Micrite limestone	90.49	Yingshan	0.709199	−0.94	−8.37	27.01
S65	5727.29	S65-3	Micrite limestone	276.29	Yingshan	0.711374	−1.8	−9.6	6.31
S65	5732.24	S65-2	Calcite in cavities	281.24	Yingshan	0.709283	−2.08	−11.03	0.61
S65	5732.24	S65-2	Micrite limestone	281.24	Yingshan	0.70902	−2.95	−10.82	0.99
S65	5733.21	S65-1	Micrite grainstones	282.21	Yingshan	0.7089	−3.13	−9.06	0.76
S65	5733.21	S65-1	Calcite in cavities	282.21	Yingshan	0.709255	−0.54	−11.01	0.76
S88	6159.73	S88-8	Micrite grainstones	675.73	Yingshan	0.709071	−2.37	−8.26	32.41
S88	6372	S88-5	Dolomite	888.00	Penglaiba	0.709682	−2.38	−8.49	71.43
S88	6408.79	S88-4	Calcite in cavities	924.79	Penglaiba	0.709258	−3.96	−12.68	1.83
S88	6408.79	S88-4	Dolomite	924.79	Penglaiba	0.709125	−0.79	−5.99	87.94
S88	6421.68	S88-2	Crystalline dolomite	937.68	Penglaiba	0.709476	−1.6	−7.62	31.34
S88	6428.15	S88-1	Dolomite	944.15	Penglaiba	0.70919	−1.63	−8.66	67.17

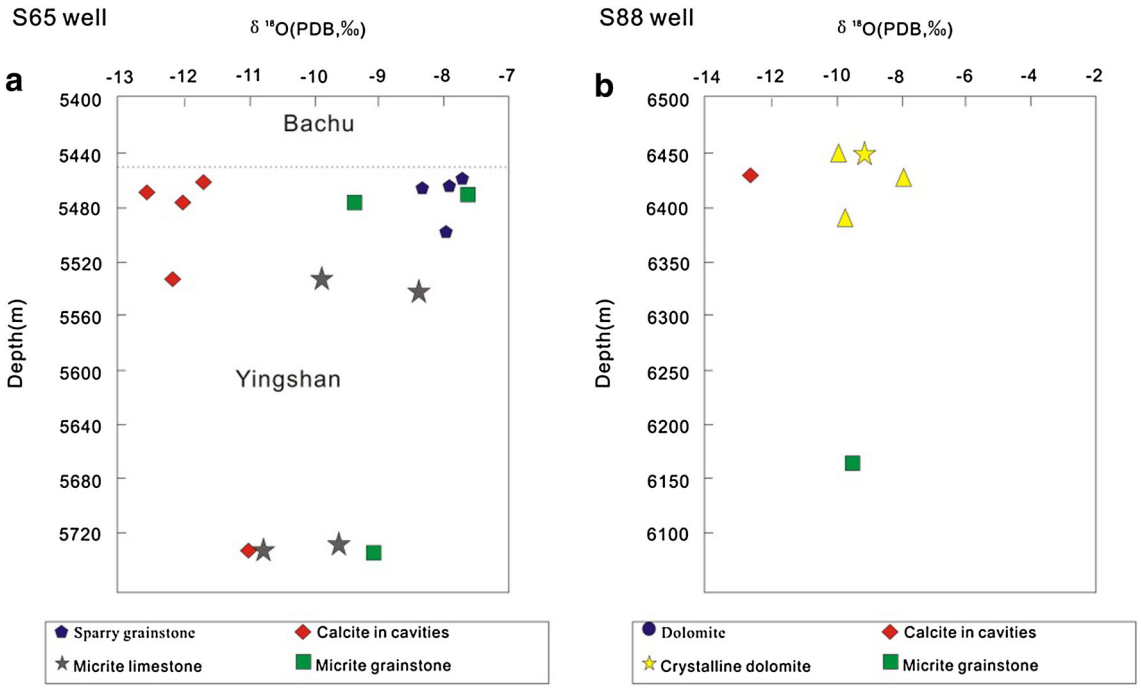

Fig. 4 Scatter plot of the oxygen isotopes of different components in the S65 and S88 wells

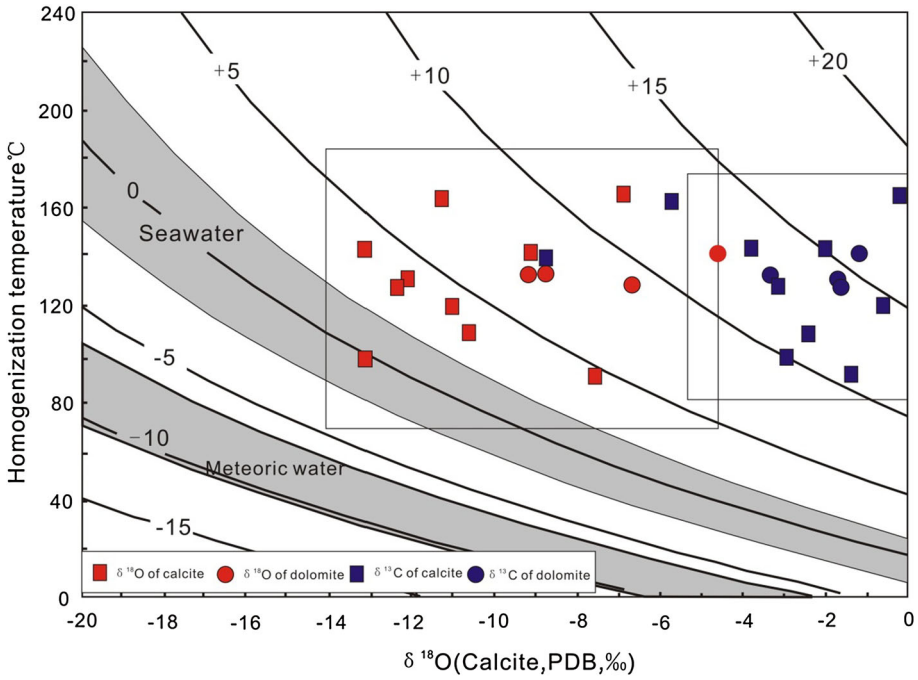

Fig. 5 The fluid inclusion homogenization temperature with carbon and oxygen isotope composition plot for Ordovician carbonates. Isoline is the oxygen isotope of fluids (Zhang 1985). The $\delta^{18}O$ value of seawater and meteoric water is that of modern seawater (Ren et al. 2000)

indicator of high temperature fluids. In this study, the standard distribution pattern of the REEs of dolomite was mapped and some dolomite samples had a positive Eu anomaly (Fig. 6), indicating that the dolomite reservoirs of the Yingshan Formation in the Tahe area were affected by hydrothermal fluids. However, in most dolomite samples, there was a negative Eu anomaly suggesting that although the dolomite was obviously related to burial dolomitization, the fluids were not of hydrothermal origin.

$^{87}Sr/^{86}Sr$ isotopes

The $^{87}Sr/^{86}Sr$ ratio of Ordovician seawater was between 0.707854 and 0.709132 (Huang et al. 2004a, b). The

$^{87}Sr/^{86}Sr$ ratios of dolomite, calcite in cavities, sparry grainstones and micrite in Ordovician carbonate of the Tarim Basin are all higher than that of contemporary seawater. The strontium isotope ratios in calcite in cavities have notably higher $^{87}Sr/^{86}Sr$ ratios than contemporary seawater (Fig. 7, Table 5). The ^{87}Sr of continental igneous rocks is generally elevated and are from continental igneous rocks (Zhu et al. 2010); thus, the $^{87}Sr/^{86}Sr$ ratio of continental hydrothermal fluid is commonly high. These high values suggest that the diagenetic water was influenced by hydrothermal fluid.

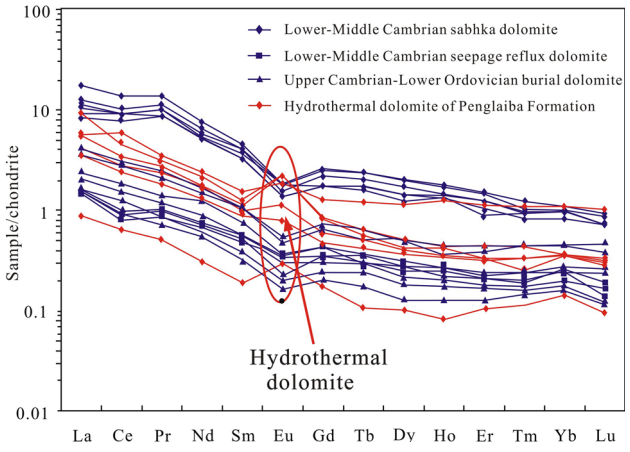

Fig. 6 REE distribution pattern of the dolomite reservoir of Tahe Oilfield, Tarim Basin

Discussions

A wide range of evidence demonstrates that deep hydrothermal fluids affected the Tarim Basin. Numerous researchers have studied the alteration and dissolution of reservoirs by hydrothermal fluids (e.g., Jin et al. 2006; Lv et al. 2007; Pan et al. 2009; Zhang et al. 2006). There are, however, few studies on the dissolution mechanism. During fluid migration, the retrograde solubility of carbonate rocks results in increased solubility as the fluid cools down and is a most effective way to enhance the dissolving capacity of carbonate minerals under deep burial conditions (Huang et al. 2010a, b). Previous studies were reviewed and data generated to address the dissolution mechanism of carbonate rocks. It was considered that carbonate rocks would dissolve under the three conditions discussed below.

Development of fault system provides the migration path for hydrothermal fluids

The saddle dolomite with high temperature features and most hydrothermal minerals such as dickite, discovered in the S88, T708, S112-1 and S76 wells, fluorite (with fluid inclusion homogenization temperatures >200 °C) in wells S85, S65, S86 and S76, and barite in well S65 are all found in the western part of the Tahe area. In this area, faults and fractures are well developed (Fig. 8). This association suggests that the migration of hydrothermal fluids and attendant mineralization might have been related to the F1

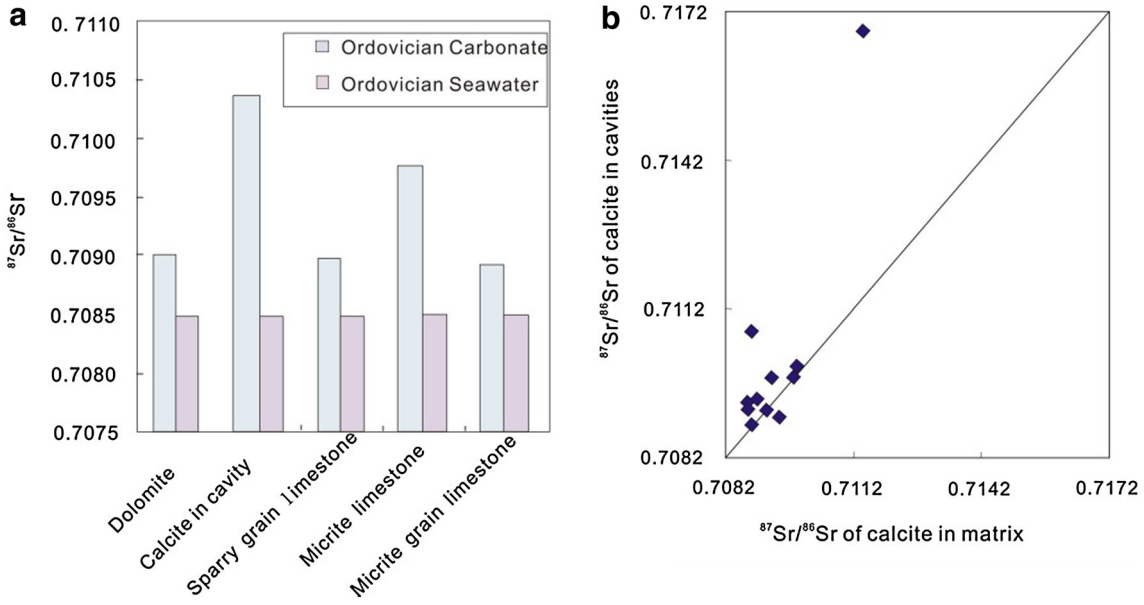

Fig. 7 Histograph of $^{87}Sr/^{86}Sr$ value in different components in the Tahe oilfield, Tarim Basin

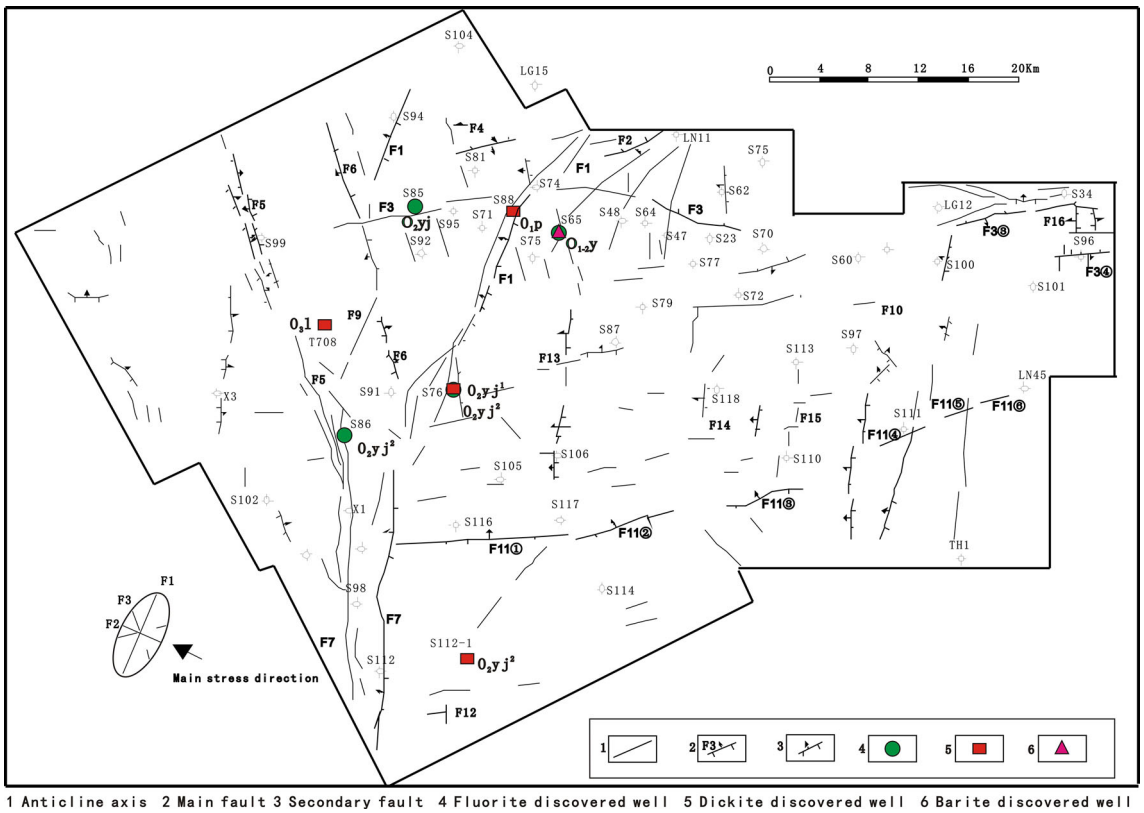

Fig. 8 Map distribution of the Ordovician fault system in the Tahe area and the hydrothermal minerals discovered in the wells

fault and associated minor faults. Hydrothermal dissolution is most prominent along the F1 and associated faults (Fig. 8).

Dissolution by hydrothermal acidic fluids

Deep acidic fluids containing large quantities of CO_2 and HF migrating through the faults are believed to be responsible for carbonate rock dissolution at shallower depth. The dissolution of carbonate rocks under deep burial conditions is believed to be associated with thermochemical sulfate reduction that could generate a large quantity of CO_2 and H_2S. The H_2S, when dissolved in water, produced H^+ and HS^-, resulting in enhanced dissolution capacity for carbonate rocks (Zhao et al. 2007, 2013).

The dissolution of grainstones and calcite in pores by strong corrosive media, such as organic acids, hydrothermal brines, and hydrogen sulfide, generally generated the matrix porosity at various scales. The matrix vuggy porosity formed due to burial dissolution was an important complement to original fractures and cavities, which significantly increased the matrix porosity of surrounding rocks. Fault-related vuggy porosity was spatially limited and predominantly occurred in the grainstones along faults and fractures.

Enhanced dissolution with temperature decrease

Hydrothermal fluids are here defined as the fluids that had temperature 5 °C or higher than surrounding rocks (Shen et al. 2010). The solubility of CO_2 and H_2S in water increases with decreasing temperature (Huang et al. 2008). Cooling of hydrothermal fluids and increased solubility of CO_2 and H_2S most likely occurred during migration of hydrothermal fluids as they ascended through faults. Therefore, when the hydrothermal fluids containing H_2S and/or CO_2 (mostly derived from thermochemical sulfate reduction (TSR) in relatively deep strata) migrated upward along faults (Fig. 9), original calcite or dolomite-saturated fluids would become unsaturated, resulting in the dissolution of calcite or dolomite in shallow formation. Thus, high-quality carbonate reservoirs should be better developed along the faults that acted as hydrothermal fluid migration pathways. However, the premise for fluid lateral migration is that the rocks with original high primary porosity and permeability, i.e., grainstones (dolomite) or

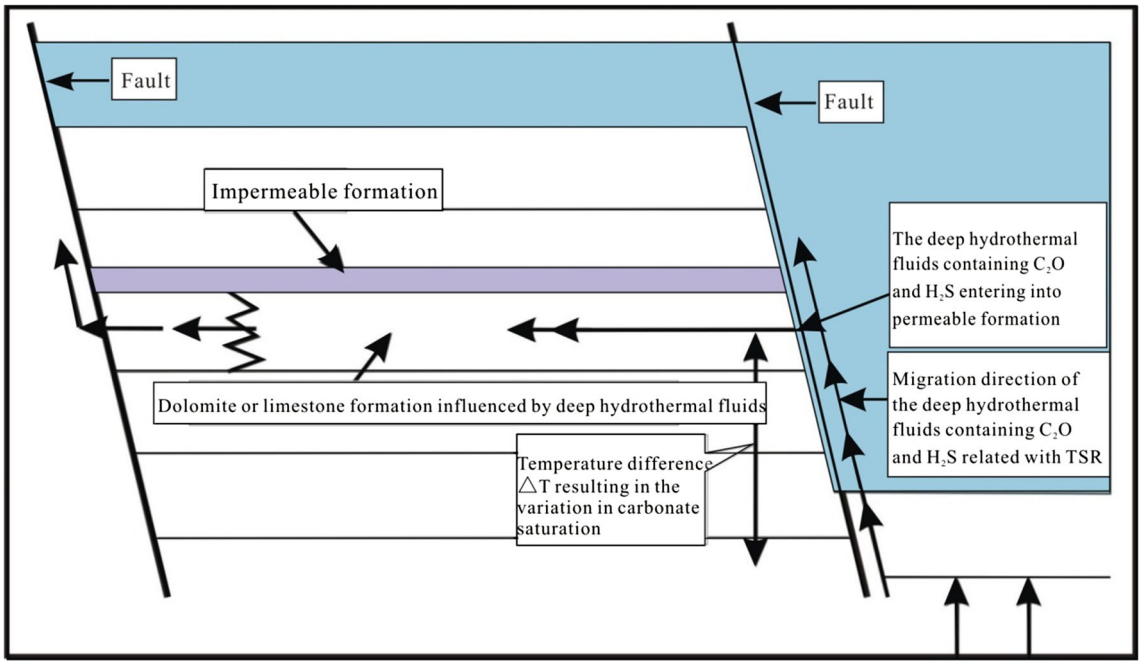

Fig. 9 Schematic diagram of the carbonate dissolution and secondary pore formation mechanism resulting from the upward and lateral migration of hydrothermal fluids containing H_2S and CO_2 (modified from Huang et al. 2008)

rudstones/framestones (dolomite), were the facies where secondary vuggy porosity would further develop during the diagenetic process.

Hydrothermal dissolution formed a series of cavities with varying sizes (Fig. 3e–h), along faults, which were generally filled or half filled by hydrothermal minerals, high temperature millimeter-scale calcite and saddle dolomite.

A large amount of shrinkage pores are formed during the formation of hydrothermal minerals

Some hydrothermal minerals could generate a large amount of shrinkage porosity, enhancing reservoir space. The occurrence of dickite played a constructive role in increasing reservoir space. Measurements of dickite and kaolinite volumes by Bish and Von (1989) and Joswig and Drits (1986) indicate that during the transformation of kaolinite into dickite, there is a 0.8 % volume reduction. If we consider the primary intercrystalline porosity of kaolinite, then the resulting intercrystalline porosity of dickite would be over 1 %, greater than that of kaolinite. This alone could account for the pervasive intercrystalline porosity associated with dickite. Furthermore, the precipitation of primary dickite from acidic fluids is generally associated with vuggy porosity in carbonate rocks. This phenomenon is also observed in the Ordovician strata in the Tahe area (Fig. 3a, d); therefore, dickite might be an indicative mineral for reservoir development or enhancement by hydrothermal fluids.

The occurrence of fluorite can also significantly improve reservoir quality. During the fluoritization of $CaCO_3$ during metasomatism, pore space relative to that of calcite would increase by 26.4 % (Liu and Cai 2009).

Conclusions

1. The analysis of mineralogical and geochemical data indicates that fluorite with high inclusion homogenization temperatures, dickite, barite and high temperature dolomite (mainly in the Penglaiba Formation) occured in the strata far away from the unconformity surface and the other Ordovician strata, indicating that deep hydrothermal fluids migrated through the Ordovician strata of the Tahe area, Tarim Basin.
2. The wells with hydrothermal minerals are mainly distributed in the west of the basin, where faults and fractures are well developed. When hot hydrothermal fluids ascended along faults, their temperature decreased making them more acidic and aggressive to carbonate rocks.
3. The evolution of hydrothermal fluids in the carbonate reservoir resulted in a large amount of fabric-selective and vuggy porosity formation. In addition,

the hydrothermal minerals, such as dolomite, fluorite and dickite, generated a large amount of shrinkage pores that contributed to increased reservoir space.

4. The dissolution of carbonate rocks caused by hydrothermal fluids generally occurred in the vicinity of fluid upward migration pathways (faults or other channels); thus, where these structures can be identified by seismic surveys or other prospecting method, we can predict that a good reservoir would be developed in the area.

Acknowledgments This research was funded by the NSF China (No. 41502062, 41202036), the China geological Survey Program (No. 1212011220762, DD20160175). We thank very much to professor Huang from Chengdu University of Technology who provides some data and samples. Dr. González of the University of Kansas, who kindly improved the manuscript are warmly acknowledged.

References

Bish DL, Von DR (1989) Rietveld refinement of the crystal structure of kaolinite. Clays Clay Min 37:289–296

Cai CF, Li KK, Cia LL, Li Band Jiang L (2009) Geochemical characteristics and origins of fracture-and vug-fillings of the Qrdovician in Tahe oilfield, Tarim Basin. Acta Petrol Sin 25(10):2399–2404

Charvet J, Shu LS, Charvet SL (2007) Paleozoic structural and geodynamic evolution of eastern Tianshan (NW China): welding of the Tarim and Junggar plates. Episodes 30:162–186

Chen RY, Zhao WZ, Zhang SC, Wang HJ (2009) The geological basis of late hydrocarbon generation and accumulation in the Lower Paleozoic of Tarim Basin. Earth Sci Front 16(4):173–181

Condie KC (1991) Another look at rare earth elements in shales. Geochem et Cosmochim Acta 55:2527–2531

Ding ZJ, Liu CQ, Yao SZ, Zhou ZG (2000) Rare earth elements compositions of high temperature hydrothermal fluids in sea floor and control factors. Adv Earth Sci 15(3):307–312

Ehrenberg SN, Nadeau PH (2005) Sandstone vs. carbonate petroleum reservoirs: a global perspective on porosity-depth and porosity-permeability relationships. AAPG Bull 89(4):435–445

Goldstein SJ, Jacobsen SB (1987) The Nd and Sr isotopic systematics of river water dissolved material Implications for the sources of Nd and Sr in seawater. Chem Geol 66:245–272

Huang SJ, Pei XG, Xie QB (1995) Dickite and its significance in Ordovician carbonate reservoir of Shaanganning Basin. J Chengdu Inst Tech 22(3):43–51

Huang SJ, Liu SG, Li GR, Zhang M, Wu WH (2004a) Strontium isotope composition of marine carbonate and the influence of diagenetic fluid on it in Ordovician. J Chengdu Univ Tech (Science & Technology Edition) 31(1):1–7

Huang SJ, Shi H, Shen LC, Zhang M, Wu WH (2004b) The global comparison of strontium isotope curve and marine strata dating in late Cretaceous in Tibet. Sci China Ser D Earth Sci 34(4):335–344

Huang SJ, Wang CM, Huang PP, Zou ML, Wang QD, Gao XY (2008) Scientific research frontiers and considerable questions of carbonate diagenesis. J Chengdu Univ Tech 35(1):1–10

Huang SJ, Tong HP, Liu LH, Hu ZW, Zhang XH, Huan JL, Huang KK (2009) Petrography, geochemistry and dolomitization mechanisms of Feixianguan dolomites in Triassic, NE Sichuan, China. Acta Petrol Sin 25(10):2363–2372

Huang SJ, Gong YC, Huang KK, Tong HP (2010a) The influence of burial history on carbonate dissolution and precipitation—a case study from Feixianguan formation of Triassic, NE Sichuan and Ordovician carbonate of Northern Tarim Basin. Adv Earth Sci 25(4):381–390

Huang SJ, Huang PP, Huang KK, Tong HP, Zhang XH, Huan JL, Liu LH (2010b) Chemical thermodynamics foundation of retrograde solubility for carbonate: solution media related to H_2S and Comparing to CO_2. Acta Sedimentaol Sin 28(1):1–9

Ihsan S, Aasm AL (2002) Multiple fluid flow events and the formation of saddle dolomite-case studies from the Middle Devonian of the Western Canada Sedimentary Basin. Mar Pet Geol 19:209–217

Jay MG, Kevin LS (1989) Geochemical and pereographic evidence for fluid sources and pathways during dolomitization and lead-zinc mineralization in southeast Missouri: a review. Carbonates Evaporites 4(2):153–175

Jin ZJ, Zhu DY, Hu WX et al (2006) Geological and geochemical signatures of hydrothermal activity and their influence on carbonate reservoir beds in the Tarim Basin. Acta Geol Sin 80(2):245–253

Joswig W, Drits VA (1986) The orientation of the hydroxyl groups in dickite by X-ray diffraction. Neues Jahrbuch für Mineralogie, Monatshefte 1:19–22

Kang YZ (2005) Cases of discovery and exploration of marine fields in China (part4): Tahe Oilfield in Tarim Basin. Marin Orig Pet Geol 10(4):31–38

Li KK, Cai CF, Cai ML, Zhang CM (2008) Hydrothermal fluid activity and thermochemical sulfate reduction in the Upper Ordovician, Tazhong area. Oil Gas Geol 29(2):217–222

Liu XF, Cai ZX (2009) Element Geochemistry Characteristics of Karstic Cave Deposit in Tahe Oilfield and Its Environmental Significance. Geol Sci Tech Inf 28(3):53–57

Liu JY, Yang HJ, Yang YP, Cai ZZ, Liu YQ, Rui ZF, Su ZZ (2012) The U-Pb chronologic evidence and sedimentary responses of Silurian tectonic activities at northeastern margin of Tarim Basin. Sci China Earth Sci 55:1445–1460

Lv XX, Xie QL, Yang N et al (2007) The carbonate oil and gas accumulation transformed by deep fluid in Tarim Basin. Sci Bull 52(S1):142–148

Ma YS, Cai XY, Zhao PR (2011) The research status and advance in porosity evolution and disgenesis of deep carbonate reservoir. Earth Sci Front 18(4):181–192

Machel HG (2005) Sedimentary rocks/dolomites. Encycl Geol 30(4):79–94

Pan WQ, Liu YF, Dickson JA (2009) The geological model of hydrothermal activity in outcrop and the characteristics of carbonate hydrothermal karst of lower Paleozoic in Tarim Basin. Acta Sedimentol Sin 27(5):983–994

Pan WQ, Hu XF, Liu YL, Gao QD, Ye Y (2012) Geological and geochemical evidences for two sources of hydrothermal fluids found in Ordovician carbonate rocks in northwestern Tarim Basin. Acta Petrol Sin 28(8):2515–2524

Ren JG, Huang YP, Fang ZS, Wang XB (2000) Oxygen and hydrogen isotope composition of meteoric water in the tropical West Pacific Ocean. Acta Oceanol Sin 22(5):60–64

Shen AJ, Pan WQ, Zhen XP, Zhang LJ, Qiao ZF, Mo NY (2010) Types and characteristics of Lower Palaeozoic Karst reservoirs in Tarim Basin. Marin Orig Pet Geol 15(2):20–29

Wang SM, Jin ZJ, Xie QL (2004) Transforming effect of deep fluids on carbonate reservoirs in the Well TZ45 region. Geol Rev 50(5):543–547

Wu DH, Li QM, Xiao ZY, Li HH, Zhang LJ, Zhang XJ (2009) The evolution characteristics of Palaeo-uplift in Tarim Basin and its exploration directions for oil and gas. Geotecton et Metallog 33(1):124–130

Wu GH, Yang HJ, Qu TL, Li HW, Luo CS, Li BL (2012) The fault system characteristics and its controlling roles on marine carbonate hydrocarbon in the Central uplift, Tarim Basin. Acta Petrol Sin 28(3):793–805

Ye DS (1994) Deep dissolution of Cambrian-Ordovician carbonates in the Northern Tarim Basin. Acta Sedimentol Sin 12(1):66–71

Yu RL (2006) Influence of tectonic movement on Ordovician carbonates of Tahe oilfield. Nat Gas Explor Dev 29(2):1–5

Zhang LG (1985) The application of the stable isotope to geology-the hydrothermal mineralization of metal activation and its prospecting. Shaanxi Science and Technology Press, Shanxi

Zhang XY, Gu JY, Luo P, Zhu PK, Luo Z (2006) Genisis of the fluorite in the Ordovician and its significance to the petroleum geology of Tarim Basin. Acta Petrol Sin 22(8):2220–2228

Zhao XY (1997) Discovery of dickite and its significance in weathering crust of lower Ordovician, Southwest depression in Tarim Basin. Xinjiang Pet Geol 18(4):4–5, 307–312

Zhao WZ, Wang ZC, Zhang S (2007) Analysis on forming conditions of deep marine reservoirs and their concentration belts in superimposed basins in China. Chin Sci Bull 52(S1):9–18

Zhao WZ, Shen AJ, Pan WQ, Zhang BM, Qiao ZF, Zheng JF (2013) A research on carbonate karst reservoirs classification and its implication on hydrocarbon exploration: cases studies from Tarim Basin. Acta Petrol Sin 29(9):3213–3222

Zhu DY, Jin ZJ, Hu WX, Zhang XF (2008) Effects of deep fluid on carbonates reservoir in Tarim Basin. Geol Rev 54(3):348–357

Zhu DY, Jin ZJ, Hu WX (2010) Hydrothermal recrystallization of the Lower Ordovician dolomite and its significance to reservoir in northern Tarim Basin. Sci China Earth Sci. 53(3):368–381

Zhu DY, Meng QQ, Hu WX, Jin ZJ (2013) Differences between fluid activities in the Central and North Tarim Basin. Geochimica 42(1):82–94